NANO LETTERS

Letter

pubs.acs.org/NanoLett

A Stable "Flat" Form of Two-Dimensional Crystals: Could Graphene, Silicene, Germanene Be Minigap Semiconductors?

A. O'Hare,[†,‡] F. V. Kusmartsev,*[,†] and K. I. Kugel[†,§]

[†]Department of Physics, Loughborough University, Leicestershire, LE11 3TU, United Kingdom

[‡]University of Glasgow, Glasgow G61 1QH, United Kingdom

[§]Institute for Theoretical and Applied Electrodynamics, Russian Academy of Sciences, Izhorskaya Street 13, Moscow, 125412 Russia

Supporting Information

ABSTRACT: The discovery of a flat two-dimensional crystal known as graphene has contradicted Landau–Peierls–Mermin–Wagner arguments that there is no stable flat form of such crystals. Here, we show that the "flat" shape of graphene arises due to a microscopic buckling at the smallest possible interatomic scale. We show that the graphene, silicene, and other two-dimensional crystals are stable due to transverse short-range displacements of appropriate atoms. The distortions are small and form various patterns, which we describe in a framework of Ising model with competing interactions. We show that when temperature decreases, two transitions, disorder into order and order into disorder, arise. The ordered state has a form of stripes where carbon atoms are shifted regularly with respect to the plane. The flat graphene, silicene, or germanene planes look like a microscopic "washboard" with the wavelength of about couple of interatomic spacing of appropriate sublattices, which for graphene is about 1.8–3.6 Å. At lower temperatures, the ordered state transforms into a glass. Because of up–down asymmetry in buckled graphene, silicene and other two-dimensional crystals deposited on substrate, a minibandgap may arise. We derive a criterion for the minigap formation and show how it is related to the buckling and to the graphene–substrate interaction. Because of the bandgap, there may arise new phenomena and in particular a rectification of ac current induced by microwave or infrared radiation. We show that the amplitude of direct current arising at wave mixing of two harmonics of microwave electromagnetic radiation is huge. Moreover, we predict the existence of miniexcitons and a new type of fermionic minipolaritons whose behavior can be controlled by the microwave and terahertz radiation.

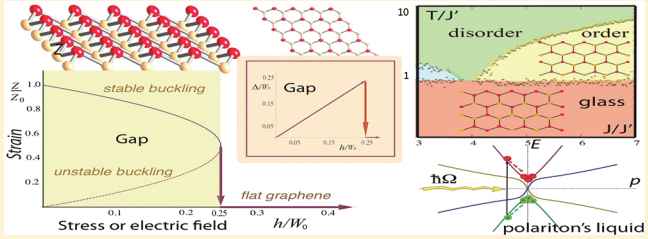

KEYWORDS: *Graphene, silicene, germanene, lattice distortions, superstructures*

Peierls and Landau proved that two-dimensional (2D) crystals are thermodynamically unstable since short-range thermal fluctuations lead to transverse atomic displacements comparable to interatomic distances.[1−3] Their arguments were later summarized as the Mermin–Wagner theorem.[4,5] Until recently, this was a common believe confirmed by many experimental observations. The discovery of graphene[6,7] shook the world. The beauty of graphene is in its 2D character and in the linear electronic energy spectrum that may lead to a very high mobility of current carriers even when impurities are present.[8]

Here, we investigate how this contradiction between the theory, comprising well-known theorems, and discovery of graphene can be resolved. Usually it is argued that 2D crystallites are quenched in a metastable state being extracted from 3D materials. Their small size (≪1 mm) and strong interatomic bonds ensure that thermal fluctuations cannot lead to the generation of dislocations or other crystal defects even at room temperature.[9] Another viewpoint is that graphene becomes stable by gentle crumpling in the third dimension on a scale of 100 Å[10] and such 3D warping leads to larger elastic energy but suppresses thermal vibrations. Here we demonstrate that there is another possibility, consistent with the Mermin–Wagner theorem. The instability in 2D leads to a formation of domains on the smallest possible scale such as interatomic spacing. Graphene, silicene, and other two-dimensional crystals as germanene may be stabilized by such short-range distortions where the neighboring atoms are shifted in the third dimension in opposite directions. Such structures are naturally arising when the effective bending rigidity vanishes that occurs for a very broad range of electron–phonon interaction.[11] We show that these 3D lattice distortions stabilize graphene, silicene, germanene, and other two-dimensional crystals while keeping its gapless band structure. We argue that these distortions in the location of carbon atoms in graphene are consistent with recent experiments[13,12] demonstrating out-of-plane displacements of carbon atoms. On the other hand, the generality of our prediction of the buckled universal shape has been revealed in recent experiments on silicene with the use of the scanning tunneling microscopy

Received: December 5, 2011
Revised: January 8, 2012

   dx.doi.org/10.1021/nl204283q | *Nano Lett.* XXXX, XXX, XXX–XXX

(STM).[14] There it was shown that the self-aligned silicene nanoribbons deposited on Ag(110) substrate have honeycomb, graphene-like buckled structure. Another clear evidence of the buckling has been identified in silicene epitaxially grown on a close-packed silver surface Ag in (111) plane.[15] There it was found a highly ordered silicon structure, arranged within a honeycomb lattice, consisting of two silicon sublattices occupying positions at different heights. The value of the sublattices displacement has been determined and is equal to 0.2 Å. (see Figure 2 in ref 15)

Already, in the molecular dynamics simulation, for example, Fasolino et al. (see Figure 3 in ref 16), it has been noticed that the bond length changes from one carbon atom to the next one. This indicates that we have changes in the interatomic spacing within the unit cell, even in the model of the flat graphene, for which the molecular dynamics simulations have been performed. In more recent first-principles calculations of structure optimization and finite temperature molecular dynamic simulations, it was shown that silicon and germanium can be stable only in two-dimensional, low-buckled, honeycomb structures (see ref 17). They have shown that planar honeycomb structures of Si and Ge are unstable toward a formation of a stable low-buckled honeycomb structures as found in the present paper. Moreover, using first-principles calculations, it was also recently shown that germanene (the germanium analogue of graphene) has the graphene-like honeycomb structure that turns out also buckled (the buckling deformation is about 0.635 Å, see ref 18). They also found that the buckled shape of germanene is more stable than the planar one and yet has an electronic structure resembling that of graphene with a linear energy dispersion around the *K*-point.

Model for the Transverse Lattice Distortions. Thus, in order to describe such atomic distortions and their configurations we use the Ising model on the 2D hexagonal lattice. Each Ising spin is related to the transverse displacement of a carbon atom in graphene or a silicon atom in silicene. Because of their elastic nature, the interactions of these Ising spins are not limited to the nearest neighbors but extend further to the next-nearest neighbors being described by two coupling constants associated with the nearest and next-nearest neighbor carbon or silicon atoms in two-dimenisonal crystals. Earlier, similar approach was applied to describe lattice distortions of the surface layer in Si.[19,20]

The two competing interactions on a square lattice lead to intrinsic frustrations and rich and unusual phase diagram.[21,22] Because of frustrations, the disordered glassy state arises from the ordered one even with decreasing temperature. Here, we show that similar effects are also relevant to graphene. At high temperatures, the shape of the graphene plane is randomly changed due to thermal fluctuations. At some lower temperatures, the out-of-plane shifts of carbon atoms are not random and form stripy patterns. However, the striking picture arises when we decrease the temperature further; there, the ordered state is again replaced by a disorder associated with a new glassy state. Graphene is stabilized by a three-dimensionality introduced by these upward and downward displacements that should alternate forming some antiferrodistortive pattern.

In principle, there may exist two types (long- and short-wavelength) of displacements. The long-wavelength fluctuations are typical for membranes and they are very likely to exist in the graphene foil. Their scale was determined only in experiment (see refs 10 and 23). In contrast to this, our main point is the existence of the short-wavelength displacements whose scale is the smallest possible one, that is, the lattice spacing. The existence of such displacement follows from the thermodynamic estimations taking into account the bandwidth, deformation potential interaction, and elastic energy. The combination of both, short- and long-wavelength fluctuations may look as a displacement of quite variable amplitude depending on the specific combination of these two. The existence of such short-range distortions does not contradict to available observations made so far.

The problem of the scale for the equilibrium transverse lattice distortions is indeed a very important one. As far as the short-wavelength distortions are concerned, it is important to note that when these transverse short-wavelength displacements arise, the most dramatic change happens with π-bonding, although both σ- and π-bondings contribute into the displacement energy. We assume here that the dominant change happens with π-bonds. In this case, the distance between carbon atoms is not changed but there appears an angle θ between neighboring bonds. That is, in this case in two-dimensional crystals the p_z–p_z overlapping increases since these orbitals are now closer to each other on a distance $r = a \cos\theta$. Because of the elongated character of these orbitals, for example, the z displacements of the order of $u_z = 0.4$ Å, will not change significantly their overlapping in z direction. Let us now make some estimates. The p_z–p_z overlapping integral can be written as

$$t_{2p\pi,2p\pi} = \exp(-r\zeta)\left[1 + r\zeta + \frac{2}{5}(r\zeta)^2 + \frac{1}{15}(r\zeta)^3\right] \quad (1)$$

where $\zeta = 3.07$ Å^{-1} and $r = 1.42$ Å for the flat graphene; see refs 24 and 25. Then, for the distorted graphene when $\sin\theta = u_z/r$ we will have new $r' = d_{\mathrm{buckl}} = 1.36$ Å. If the value of ζ slightly increases as well, the overlapping integral will not change much. Its exact value depends also on the angle between these p_z orbitals; also the σ orbitals can contribute. Therefore, the accurate estimation should include extra assumptions and other bands. For simplicity, we limit ourselves to a few assumptions to make the very rough but realistic estimation. From these estimations of the overlapping integrals, we see that the short-range distortions lead effectively to an increase of the width of the π-band. Of course, such a distortion costs the elastic energy. However, the total energy including the electronic degrees of freedom (due to the change in the bandwidth arising due to the increase in overlapping of p_z orbitals) and elastic contributions decreases. The minimum value of this energy corresponds to the equilibrium displacement u_z of carbon atoms in the transverse z-direction. An estimation gives approximately the value for these displacements as $\Delta u_z/a \approx D^2/Et$, where t is the width of the π-band, E is the elastic modulus (transverse shear), and D is the deformation potential associated with the change of the π-band due to an increase of the overlapping integral $D \sim (\partial t_{2p\pi,2p\pi})/(\partial u_z)$ and a is a distance between carbon atoms. The amplitude of these distortions increases with temperature, and eventually they lose stability. With the growth of temperature, there arise frequent transitions between different distorted configurations.

Note that the energy loss due to changing of interatomic distance due to the out-of-plane shift of carbon atoms (elastic term) could be compensated by a larger hybridization of p orbitals of neighboring carbon atoms.[26] If there are out-of-plane

dx.doi.org/10.1021/nl204283q | *Nano Lett.* XXXX, XXX, XXX–XXX

shifts of neighboring carbon atoms in opposite directions, the two neighboring p_z orbitals are overlapping more due to their elongation and the value of their matrix element increases, that is, the π-bond becomes stronger. This preserves the Dirac spectrum where the "velocity of light" just increases only.

To describe the out-of-plane glassy distortions we use the model

$$H = J \sum_{\langle i,j\rangle_{nn}} s_i s_j + J' \sum_{\langle i,j\rangle_{dn}} s_i s_j - h \sum_i s_i \qquad (2)$$

where the two-valued Ising spin variables, namely, $s_i = 1$ for an upward displacement of a carbon atom (spin up), whereas $s_i = -1$ (spin down) corresponds to the downward displacement. There are here two competing antiferromagnetic nearest-neighbor and next-nearest-neighbor interactions, J and $J' > 0$. $\langle i, j\rangle_{nn}$ and $\langle i, j\rangle_{dn}$ denote the summation over sites i and j being respectively nearest neighbors (nn) and diagonal neighbors (dn), and h is the analog of magnetic field corresponding to some external stress and determining the graphene bandgap. Since the deformation energy of each atomic distortion decreases as $1/r^3$, the J/J' ratio for graphene should be equal to $J/J' = 3^{3/2}$. This cubic decay has been discussed in the paper;[27] see, for example, eq 22 and the discussion after this equation in this cited paper.[27] There it is explicitly shown that the deformation from point sources has a cubic decay. However, our results have a broader range of applicability, namely, we discuss not only one value for the ratio J/J' associated with cubic decay but all possible values for the J/J' ratio, see the phase diagram in Figure 1. That covers any case of the asymptotic behavior and distribution of elastic strains under study.

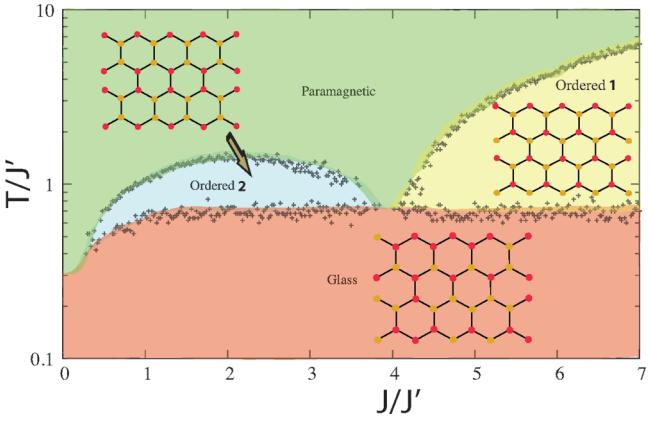

Figure 1. Phase diagram for the Ising model on a honeycomb lattice. The high-temperature phase transition is calculated from the peaks in the specific heat, while the low-temperature transition is obtained from the change in the magnetization and the analysis of a domain-wall order parameter. We see that in the temperature range between the high-temperature disordered (paramagnetic) phase and the low-temperature disordered phase (glass), there exist regularly ordered (at least, partially) stripy phases (Ordered 1 and Ordered 2). The structure of distortions (Ising spins) for the honeycomb lattice is schematically shown near the corresponding regions of the phase diagram; filled and open circles denote up and down distortions. For the Ordered 1 phase, depicted also in Figure 3, one may easily notice single stripes oriented in three equivalent directions, simultaneously. In the Ordered 2 phase, there are double stripes oriented along only one of the three possible directions. Of course, they can be oriented in any of these three directions with equal probability. This gives a possibility to form domains with different stripe ordering.

Results of Numerical Modeling. Using the methods described in refs 21 and 22, we have performed intense the transfer matrix and Monte Carlo simulations of the Ising model focusing on the graphene parameters ($J/J' = 3^{3/2} \approx 5.2$). For different 2D crystals, like silicene, forming monolayers on different substrates, the J/J' ratio can vary within a rather broad range. The calculated phase diagram in $J/J' - T/J'$ plane is given in Figure 1. There are two ordered (1 and 2) states arising at intermediate temperatures: the conventional antiferromagnetic order at $J/J' > 4$, and the double stripes at $J/J' < 4$. At low temperatures, such state is a glass, which is similar to the Ising glass described in refs 21 and 22. For graphene parameters, where ($J/J' = 3^{3/2} \approx 5.2$) the temperature evolution of the buckling structures ("snapshots") for 100 × 100 lattices is illustrated in Figure 2. The snapshot taken at very low temperatures is shown in Figure 2a. It is a very disordered state, which may be considered as an ordered state with a large number of frozen topological defects highlighted in orange and blue in the zoom-inset. The frozen defects can form a very large number of disordered configurations associated with a complicated energy landscape, where each of these configurations corresponds to a local minimum. At very low temperatures, all energy minima are separated by high barriers and therefore the disordered state and many others quasi-ordered states are locally stable. The state with such properties is a glass, which has its own order parameter (details on the glass and its order parameter see in Supporting Information).

With increasing temperature, the height of barriers decreases, defects are annealed, and the order is restored. Indeed, in Figure 2b, there are rather large domains with the stripy order shown in Figure 3. We see that the parent ideal graphene plane becomes strongly corrugated (a washboard structure). In fact, we have two triangular lattices shifted with respect to one another and with respect to the original plane. The atomic-resolution transmission electron microscopy of suspended graphene indeed sees such distortions[23,31] (see details in Supporting Information). The ordered structures forming domains with regular patterns inside are actually separated by disordered narrow regions or by boundary layers where one may expect an intermixture of numerous defects of the ordered state. Their origin is related to a proliferation of the topological defects, such as domain walls, into the ordered stripy states. The situation is reminiscent of the proliferation of topological defects in the Ising model with competing interaction on the square lattice described in refs 21 and 22. This transformation of the disordered state into ordered one arises already at the temperature $T/J' \simeq 0.1$. It is rather slow crossover. Even at the temperatures as high as $T/J' = 2.0$, the order is still not reestablished; see Figure 2b. Above $T = 2.5J'$, the out-of-plane distortions become random, and we get an analog of the paramagnetic state for the Ising spins; see Figure 2c.

Let us estimate the characteristic energy of a buckling defect for the state "Ordered 1"; see Figure 1. The Young modulus of graphene is $E = 0.5-1$ TPa.[32,33] The usage of this Young's modulus in the estimates gives only an order of magnitude for the physical quantities and may be considered as an upper limit. In reality, of course, existing values for a transverse shear should be smaller by an order of magnitude (see ref 28). This is because the main contribution is coming from the π-bonding. Then, the upper limit for the work performed to produce an out-of-plane displacement Z_0 (see, Figure 3) of a single atom,

dx.doi.org/10.1021/nl204283q | Nano Lett. XXXX, XXX, XXX−XXX

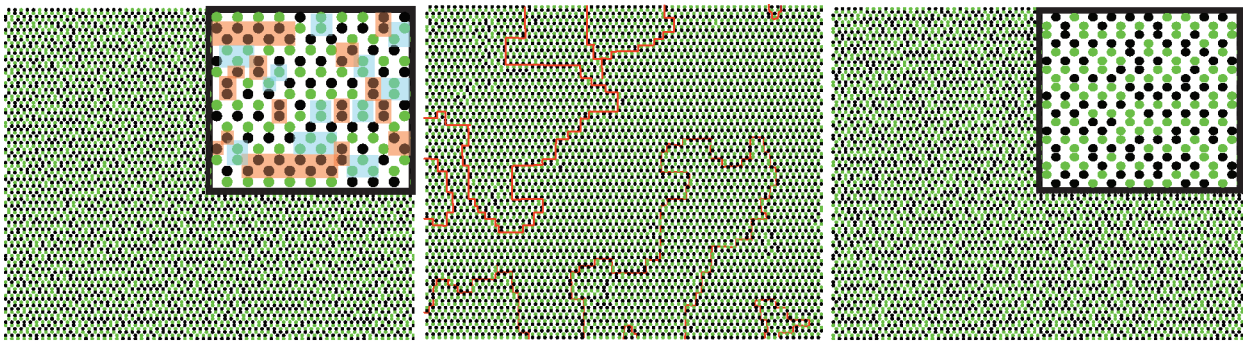

(a) $T/J' = 0.02$ (b) $T/J' = 2.0$ (c) $T/J' = 5.0$

Figure 2. Snapshots of the superstructures formed on a honeycomb graphene lattice ($J/J' = 3^{3/2}$) at various temperatures, where black and green dots denote the up and down displacements of carbon atoms. (a) Glass, a disordered state at low temperatures that is formed by a large number of topological defects. Inset shows a magnified portion of this snapshot with numerous frozen defects. They are two long zig-zags marked by orange, where neighboring atoms are displaced together in the same directions, buckled up. There are three shorter zig-zags buckled down and marked blue. Also, there are many pairs buckled up and down. For freely suspended graphene, the numbers of atoms buckled up and down are equal. (b) The ordered state. With increasing temperature, the structure of the out-of-plane atomic displacements becomes partially ordered. The strict antiferrodistortive order presented in Figure 3 exists only within large domains. The domain boundaries are filled with many pairs of defects and are denoted by red solid lines. Such state exists only at the intermediate temperature range and disappears at high temperatures; see the phase diagram in Figure 1. (c) An instantaneous snapshot of a disordered high-temperature structure. It consists of many short-range defects (pairs) whose creation is dictated by thermal fluctuations. Its form changes with characteristic times associated with optical phonon frequencies. A magnified portion of this snapshot does not reveal any traces of regularity.

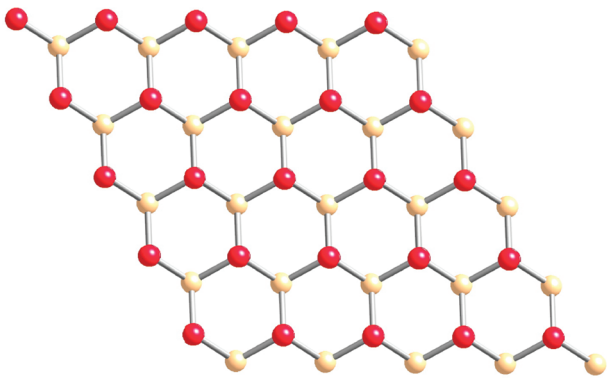

(a) Top view

(b) Side view

Figure 3. Washboard structure of graphene. Yellow and red spheres correspond to carbon atoms shifted downward and upward with respect to the initial plane, respectively. Each atom and its three nearest neighbors form a tetrahedron with the base side in the plane d_{buckl} and height $u_z = Z$.

which forms a tetrahedron with its three neighbors, is $W_0 = p\Delta V$, where $\Delta V = [(3)^{1/2}Z_0^3]/32$ is a volume change per atom due to the buckling and p is an applied pressure.

Following the data for graphene reported recently in ref 13, we take the period, $d_{buckl} = 1.8$ Å (see Figure 3) and determine $Z_0 = 0.95$ Å. If $p = E$, we obtain $W_0 = 0.135-0.27$ eV. According to our model, $W_0 = 6J - 12J'$. Hence we have $J \simeq 0.035-0.07$ eV and $J' = 0.007-0.014$ eV. Therefore, according to the phase diagram in Figure 1, at the temperature $T = 0.5J' \simeq 35-70$K, there arises a transition to a glass state. The state Ordered 1 exists between $0.5J' < T < 2.5J'$, that is, it vanishes only above $T \simeq 175-350$ K, where thermal fluctuations dominate. For silicene the Ordered 1 should vanish already above $T \simeq 70$ K because its elastic modulus for silicene can be approximately by a factor of 5 smaller than for graphene. For example, in the harmonic approximation the elastic force constants calculated with the use of the first-principles density-functional theory[29] for armchair graphene, silicene, and BN nanoribbons are equal to 176, 30, and 144 N/m, respectively.

Bandgap Formation Due to Graphene–Substrate Interaction and External Electric Field. These estimations change when we consider graphene, silicene, or germanene on a substrate. For example, when we have considered the suspended graphene, the transverse lattice distortions have no effect on the Dirac K and K' points of the Brillouin zone. These points are invariant when there is no symmetry breaking between up and down displacements. However, if there is a substrate, this will give rise to some force (including the van der Waals ones), which should be different for atoms taking part in up and down transverse displacements. Using the method of invariants of the crystal groups developed in the framework of the $k-p$ methods (see, for example, the book in ref 30), we can arrive at the magnetic-field-like term, which has the form $\sigma_z h$. This term is an invariant with respect to the graphene crystal symmetry group. Then with this term, the symmetry between the up and down out-of-plane displacements is breaking and the gap Δ in the graphene spectrum may be open.

Thus, we obtain its value from the Dirac Hamiltonian $H = \hbar v_F \vec{k}\,\vec{\sigma} - h\sigma_z$ associated with one valley only, where h describes a stress induced by substrate and is the analog of magnetic field from the Ising model, eq 2. The resulting spectrum is $\varepsilon(k) = \pm$

dx.doi.org/10.1021/nl204283q | Nano Lett. XXXX, XXX, XXX–XXX

$(v_F^2\hbar^2k^2 + h^2)^{1/2}$; this gives the gap $\Delta = 2h$. With the stress h induced by a substrate, the energy balance is described by the equation $W_0s^3 = W_0s^2 - hs$. The solution of this equation gives the dependence of the dimensionless buckling amplitude $s = Z/Z_0$ (an effective strain) on the substrate-induced stress, h. So, we have $Z = Z_0\{1/2 \pm [1/4 - (h/W_0)]^{1/2}\}$. When $h \leq W_0/4$, for each value of h there are two solutions here: one is stable and associated with large buckling amplitude, the other one associated with smaller buckling amplitude is unstable. When $h > W_0/4$, the buckled state disappears and there is only state corresponding to a flat graphene with the gapless electron spectrum (see, Figure 4). Probably, such situation arises for graphene on mica substrate[34] or on a graphene membrane, which conforms to the atomically flat h-BN.[35] By an appropriate choice of the substrate, one may reach the maximum bandgap equal to $\Delta_{max} = W_0/2$ (see, the inset in Figure 4).

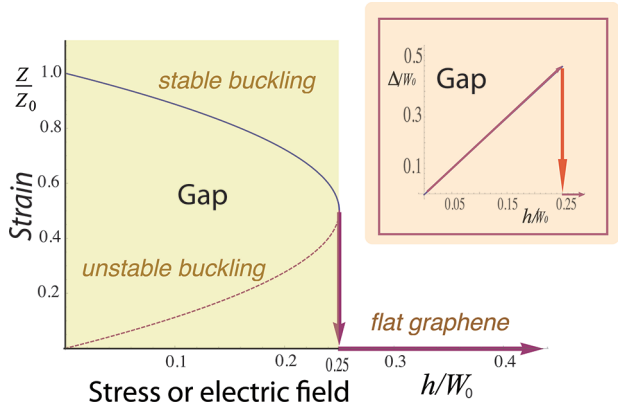

Figure 4. Buckling amplitude Z (effective strain) versus transverse stress, h, which may be produced by a substrate or by an application of a transverse electric field $h \sim E_z$. The region when the gap arises is indicated by the yellow color. The transverse stress from the substrate or from a transverse electric field leads to the breaking of the symmetry between up and down out-of-plane displacements of carbon, Si or Ge atoms, respectively and, therewith, to the opening of a bandgap Δ in their energy spectrum. For suspended graphene as for others 2D crystals, we have two possible states: unstable flat graphene with $Z = 0$ and stable buckled graphene with $Z = Z_0$. With increasing the stress, the bandgap increases while the buckling amplitude decreases. The stable buckling amplitude reaches its minimum value, $Z = Z_0/2$, at $h = W_0/4$, where W_0 is an elastic energy of the equilibrium buckled state in suspended graphene normalized per single carbon atom. As the stress increases further, the buckled state turns out to be unstable and graphene exists only in a flat form. For the buckled state, the bandgap increases with the stress linearly $\Delta = 2h$, see the inset. At the critical distortion $Z = Z_0/2$ or the critical stress $h = W_0/4$, the bandgap drops to zero. Of course, with a further increase of the stress h, in the flat graphene the bandgap vanishes (see inset). This sharp transition is indicated by vertical arrow both in the main panel and inset. As we can see in the inset, the maximum value of the bandgap is $\Delta = W_0/2$. According to our estimates, $W_0 = 0.13 - 0.26$ eV and hence $\Delta = 0.065 - 0.13$ eV. So, the bandgap induced by various substrates may be changed in a broad range, which is, however, limited by an onset of the buckling instability.

The formation of the minigap in two-dimensional crystals such as graphene, silicene, germanene, or any 2D crystals is one of the main predictions of this paper. An existence of such minigap has not been confirmed yet in experiment. Such minigap will arise only at some specific conditions, which can be created by a choice of substrate. In some cases, like in BN case,[35] the substrate acts so strongly on graphene that all transverse displacements vanish at low temperatures and the buckled shape flattens. In this case, we predict the absence of the minigap. In the other case, for example, when graphene was formed on a graphite or other substrate weakly bound with graphene deposited on the top, the mingap might be formed. According to our estimations, its value may be approximately ranging from 10 to 40 meV.

Wave Mixing and dc Current Generation. It is important to note that an application of a transverse electrical field of the amplitude E_z can be described by the same invariant term in the Hamiltonian as $\sigma_z h_E$, where the value $h_E = E_z u_z$. The application of the field E_z can provide an additional force to an substrate and may be an additional tool to form a minigap. For example, by an application of the electric field, one may change the value h to $h \rightarrow h + h_E$ and increase or decrease the degree of the buckling u_z or the value of the minigap Δ. In fact the value of the minigap changes dramatically in the vicinity of the critical h_c equal to $h_c = W_0/4$ when the minigap has a maximum (see Figure 4). Thus, if the gapless 2D crystal such as graphene, silicene, or BN is located in the vicinity of the critical point described by the red vertical arrow on the Figure 4, then even by an application of a small transverse electric field a minigap as large is 40 meV can be created. Thus, the application of the transverse electric field to different two-dimensional crystals such as the buckled graphene, silicene, and germanene may open a bandgap, which value may be changed both linearly and nonlinearly with a change of the strength of electric field. The linear dependence of the minibandgap value on the strength of electric field arises for suspended 2D crystals. The nonlinear sharp switching of the minigap may arise on the 2D crystals deposited on some substrates, where $h = h_c$. Such sharp switching of the minibandgap by electric field may be used in different electronic devices such as field effect transistors made from the 2D crystals.

When the minigap exists, a new effect of the generation of direct current may arise as well. The effect is, in essence, due to a nonlinearity or nonparabolicity of the electron−hole energy bands in the mini-gapped graphene and occurs mainly at a mixing of coherent electromagnetic radiations of commensurate frequencies. In the past, the similar effect has been discussed in semiconductor superlattices and III−IV type semiconductors.[36] It is stronger in systems where this nonparabolicity is larger. The energy spectrum in the mini-gapped graphene has a strong nonlinearity and nonparabolicity. Therefore, we expect here a strong generation of direct current arising at wave mixing of two harmonics of microwave electromagnetic radiation: $E = E_1 \cos(\Omega t) + E_2 \cos(2\Omega t + \phi_2)$, where E_1 and E_2 are the amplitudes of the first and second harmonics, respectively, oriented parallel to the graphene plane, Ω is the frequency. The relative shift of phases between waves is ϕ_2. Indeed, our estimations indicate that, in the particular case of the mini-gapped graphene, the amplitude of the rectified current per unit area j_{dc} is equal to $j_{dc} \approx env_F^4(eE_1)^2eE_2 \cos(\phi_2)/(\Omega^3h^3)$. Here, n is the density of electrons or holes, which may be controlled by a gate voltage. If we put in this equation the estimated minigap value, $h = 100$ meV, the electron density, $n \approx 10^{16}$ cm^{-3}, the electric field amplitudes $E_1 \sim E_2 \sim 100$ V/cm, and the frequency 1 THz, we get a very large DC current density $j_{dc} \sim 10^6$ A/m^2. The obvious causes of the huge effect are small values of the minigap, $\Delta = 2h$, and a large amplitude of the second harmonic, which can be comparable in graphene with the first one.[37] The effect is stronger when the minigap and the

dx.doi.org/10.1021/nl204283q | Nano Lett. XXXX, XXX, XXX−XXX

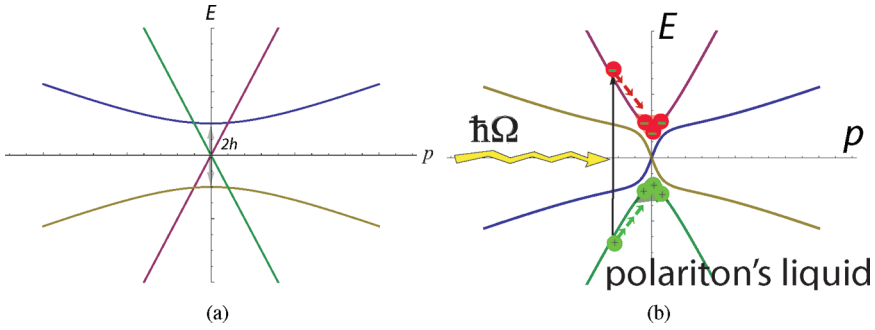

Figure 5. (a) The Dirac gapless spectrum of microwave photons (see, the red and green lines) and minisemiconducting spectrum of electrons and holes in graphene (see, blue and brown parabolic-like curves) with the minigap $\Delta = 2h$ when Coulomb interaction between electrons and photons has not been taken into account. (b) The polariton spectrum in the same system when electron-photon interaction has been taken into account. Because of electron− or hole−photon hybridization, there arise two types of polariton branches. For the first type of polariton excitations, the gap disappears and the Dirac-like spectrum reinstalled. While for the second type of excitations there arise two polariton minima, that is these polaritons have the parabolic energy momentum relations. In other words, these polaritons are massive and have a charge corresponding to both electrons and holes from which they have been originated. The microwave pumping of graphene in a cavity may lead to an accumulation of the electron- and hole-polaritons in the bottom of the appropriate electron− and hole−polariton bands. There, two types of mini-polaritons may coexist and interact. The Coulomb interaction between these electron− and hole−polaritons may lead to a formation of electron−hole polariton (EHP) liquid indicated by the red and green droplets on the Figure. The gap is shrinking due to the EHP condensation energy. These polaritons are charged and therefore there may arise interesting phenomena related to their Coulomb interaction when their density changes. There, due to electron−phonon interaction the minipolaritons may be paired to form bosons. Then, depending on their coherence length a Cooper pairing or a Bose condensation of such boson mini-polaritons may also arise, where a critical temperature will depend on their density.

frequency of the mixing harmonics smaller. However, even in the optical range the graphene is an ideal target for multiple harmonics mixing. Indeed, strong effects of four-harmonics mixing measured in optical and far-infrared range have been recently observed in graphene[38] (which is by 8 orders of magnitude larger than that of the conventional insulating glass material) confirming our main conclusions.

Electron−Hole Liquid of Polaritons. Here, special attention should be given to an existing strong interaction between microwave radiation and electrons and holes, which may be caused in graphene by the same electromagnetic radiation. If there is no such interaction, the spectra of the minigapped graphene and photons are intersecting; see Figure 5a. Because of electron−photon interaction, the level crossing vanishes (anticrossing theorem) and new polariton branches arise; see Figure 5b. Note that typically a polariton in semiconductors arises due to the mixing of an infrared photon with an excitation of a material such as an optical phonon or exciton. Here, we propose a new type of polaritons resulting from coupling of microwave or terahertz photon with the electron−hole spectrum of the mini-gapped graphene. The energy of the microwave photons taking part in a formation of such minipolaritons is significantly lower than of the infrared photons used in typical polariton experiments and therefore we expect the properties of the mini-polaritons will be significantly different. In particular, they may be more easily controlled for graphene films embedded within microwave resonators.

Moreover, the spectrum of the upper polariton branch, $\varepsilon(k) = (c^2\hbar^2k^2 + h^2)^{1/2}$ has a slope, which is by two orders steeper than that of the spectrum for the for minigapped graphene, since the speed of light in graphene $c \gg v_F$; see, Figure 5b. In the estimation of the speed of light in graphene c, we used the refractive index $n_r \approx 2.6$ measured in ref 39. Therefore, at the presence of polaritons the strong rectification effects discussed above enhanced even more $\sim c^4/v_F^4$. Of course, at the presence of polaritons various many-body effects and their kinetics and decay should be taken into account. To accumulate the mini-polaritons, graphene should reside in a resonator. In such a case, at low temperatures the polaritons may form superfluids associated with their Bose condensates. The lifetime of such superfluids may be very long depending on the quality factor of the resonator.

Conclusion. In conclusion, we have found that any two-dimensional crystal such as graphene, silicene, germanene, BN or any other can be stabilized by short-range (maybe disordered) structures consisting of the transverse atomic displacements. The predicted shape of graphene looks like a lattice of cages or a regular antiferrodistortive stripy pattern with the period $\lambda \sim 1.8$ Å or 3.6 Å, or larger.

There are interesting and readily observable signatures of the buckling transitions proposed in Raman and infrared experiments. We expect that there should exist a double splitting of some Raman lines (like the D or G lines). However due to their broadness of these spectral lines such splitting is difficult to observe since. It may be small and needed to be carefully separated out in the Raman studies. In general, the Raman signal is taken from a large area and the distortions are random that leads to the involvement of the strong dispersion of the Raman lines. However, the frequencies of the phonons, associated with $E_{2g} - \Gamma$ and $A' - K$ Raman modes from the highest optical phonon band can be used to probe the amplitude of such buckling. The dependence of these frequencies on the amplitude of the buckling for silicene has been estimated in a very recent paper.[40]

Graphene or any two-dimensional crystal such as BN, silicene, or germanene deposited onto a substrate can exhibit a minibandgap due to a symmetry breaking between up and down out-of-plane atomic displacements. The formation of such a gap can be also switched or its value changed by a transverse electrical field. This provides a possibility to control the bandgap by a choice of substrate and investigate new phenomena, which may arise in such easily formed minibandgap two-dimensional semiconductors.

dx.doi.org/10.1021/nl204283q | Nano Lett. XXXX, XXX, XXX−XXX

■ ASSOCIATED CONTENT

Supporting Information

The numerical Monte Carlo modeling of the transverse lattice distortions and the formation of the buckling superstructures in a single graphene layer as well as the details for the given phase diagram are presented. This material is available free of charge via the Internet at http://pubs.acs.org.

■ AUTHOR INFORMATION

Corresponding Author

*Phone: +44-1509-223316. Fax: +44-1509-223986. E-mail: F. Kusmartsev@lboro.ac.uk.

■ ACKNOWLEDGMENTS

We are grateful to Eva Andrei, A. Boris, A. Balanov, Marat Gaifullin, Gilles Montambaux, F. M. Peeters, and Jurgen H. Smet for useful discussions. The work was supported by the ESF network-program AQDJJ, the Royal Society of London (Grant JP 090710), and the Russian Foundation for Basic Research (Projects 10-02-92600-KO and 11-02-00708).

■ REFERENCES

(1) Peierls, R. E. Quelques propriétés typiques des corpses solides. *Ann. Inst. H. Poincaré* **1935**, *5*, 177−222.
(2) Landau, L. D. Zur Theorie der Phasenumwandlungen II. *Phys. Z. Sowjetunion* **1937**, *11*, 26−35.
(3) Landau, L. D.; Lifshitz, E. M. *Statistical Physics, Part I*, Pergamon Press: Oxford, 1980; Sections 137 and 138.
(4) Mermin, N. D.; Wagner, H. Absence of ferromagnetism or antiferromagnetism in one- or two-dimensional isotropic Heisenberg models. *Phys. Rev. Lett.* **1966**, *17*, 1133−1136.
(5) Mermin, N. D. Crystalline order in two dimensions. *Phys. Rev.* **1968**, *176*, 250−254.
(6) Novoselov, K. S.; Geim, A. K.; Morozov, S. V.; Jiang, D.; Zhang, Y.; Dubonos, S. V.; Grigorieva, I. V.; Firsov, A. A. Electric field effect in atomically thin carbon films. *Science* **2004**, *306*, 666−669.
(7) Novoselov, K. S.; Jiang, D.; Schedin, F.; Booth, T. J.; Khotkevich, V. V.; Morozov, S. V.; Geim, A. K. Two-dimensional atomic crystals. *Proc. Natl. Acad. Sci. U.S.A.* **2005**, *102*, 10451−10453.
(8) Kusmartsev, F. V.; Tsvelick, A. M. Quasimetallic properties of heterojunction. *Pis'ma Zh. Eksp. Teor. Fiz.* **1986**, *42*, 207 [*Sov. Phys. JETP Lett.*, **1986**, **42**, 257. This may have been the first work where topological insulators and how they could be made was discussed.
(9) Geim, A. K. Graphene: status and prospects. *Science* **2009**, *324*, 1530−1534.
(10) Meyer, J. C.; Geim, A. K.; Katsnelson, M. I.; Novoselov, K. S.; Booth, T. J.; Roth, S. The structure of suspended graphene sheets. *Nature* **2007**, *446*, 60−63.
(11) San-Jose, P.; González, J.; Guinea, F. Electron-induced rippling in graphene. *Phys. Rev. Lett.* **2011**, *106*, 045502.
(12) Luican, A.; Li, G.; Reina, A.; Kong, J.; Nair, R. R.; Novoselov, K. S.; Geim, A. K.; Andrei, E. Y. Single layer behavior and its breakdown in twisted graphene layers. *Phys. Rev. Lett.* **2011**, *106*, 126802.
(13) Mao, Y.; Wang, W. L.; Wei, D.; Kaxiras, E.; Sodroski, J. G. Graphene structures at an extreme degree of buckling. *ACS Nano* **2011**, *5*, 1395−1400.
(14) Aufray, B.; Kara, A.; Vizzini, S.; Oughaddou, H.; Leandri, C.; Ealet, B.; Le Lay, G. Graphene-like silicon nanoribbons on Ag(110): A possible formation of silicene. *Appl. Phys. Lett.* **2010**, *96*, 183102.
(15) Lalmi, B.; Oughaddou, H.; Enriquez, H.; Kara, A.; Vizzini, S.; Ealet, B.; Aufray, B. *Appl. Phys. Lett.* **2010**, *97*, 223109.
(16) Fasolino, A.; Los, J. H.; Katsnelson, M. I. Intrinsic ripples in graphene. *Nat. Mater.* **2007**, *6*, 858−861.
(17) Cahangirov, S.; Topsakal, M.; Aktürk, E.; Sahin, H.; Ciraci, S. Two- and one-dimensional honeycomb structures of silicon and germanium. *Phys. Rev. Lett.* **2009**, *102*, 236804.
(18) Behera, H.; Mukhopadhyay, G. First-principles study of structural and electronic properties of germanene. *AIP Conf. Proc.* **2011**, *1349*, 823−824.
(19) Inoue, K.; Morikawa, Y.; Terakura, K.; Nakayama, M. Order-disorder phase transition on the Si(001) surface: Critical role of dimer defects. *Phys. Rev. B* **1994**, *49*, 14774−14777.
(20) Pillay, D.; Stewart, B.; Shin, C. B.; Hwang, G. S. Revisit to the Ising model for order-disorder phase transition on Si(0 0 1). *Surf. Sci.* **2004**, *554*, 150−158.
(21) O'Hare, A.; Kusmartsev, F. V.; Kugel, K. I.; Laad, M. S. Two-dimensional Ising model with competing interactions and its application to clusters and arrays of π-rings and adiabatic quantum computing. *Phys. Rev. B* **2007**, *76*, 064528.
(22) O'Hare, A.; Kusmartsev, F. V.; Kugel, K. I. Two-dimensional Ising model with competing interactions: Phase diagram and low-temperature remanent disorder. *Phys. Rev. B* **2009**, *79*, 014439.
(23) Meyer, J. C.; Kisielowski, C.; Erni, R.; Rossell, M. D.; Crommie, M. F.; Zettl, A. Direct Imaging of Lattice Atoms and Topological Defects in Graphene Membranes. *Nano Lett.* **2008**, *8*, 3582−3586.
(24) Hansson, A.; Stafström, S. Intershell conductance in multiwall carbon nanotubes. *Phys. Rev. B* **2003**, *67*, 075406.
(25) Mulliken, R. S.; Rieke, C. A.; Orloff, D.; Orloff, H. Formulas and numerical tables for overlap integrals. *J. Chem. Phys.* **1949**, *17*, 1248−1267.
(26) Castro Neto, A. H.; Guinea, F.; Peres, N. M. R.; Novoselov, K. S.; Geim, A. K. The electronic properties of graphene. *Rev. Mod. Phys.* **2009**, *81*, 109−162.
(27) Kusmartsev, F.V.; Rashba, E.I. Self-trapping from degenerate bands (spin S=1)and related phenomena. *Zh. Eksp. Teor. Fiz.* **1984**, *86*, 1142, [*Sov. Phys. JETP* **1984**, **59**, 668].
(28) (a) Yang, X. X.; Li, J. W.; Zhou, Z. F.; Wang, Y.; Yang, L. W.; Zheng, W. T.; Sun, C. Q. Raman spectroscopic determination of the length, strength, compressibility, Debye temperature, elasticity, and force constant of the C-C bond in graphene. *Nanoscale* **2012**, *4*, 502−510. (b) Kolosov, O.; Falko, V. et al. Private communication, 2011.
(29) Topsakal, M.; Ciraci, S. Elastic and plastic deformation of graphene, silicene, and boron nitride honeycomb nanoribbons under uniaxial tension: A first-principles density-functional theory study. *Phys. Rev. B* **2010**, *81*, 024107.
(30) Bir, G. L.; Pikus, G. E. Symmetry and strain induced effects in semiconductors; Wiley: New York, 1974.
(31) *Science Daily*, Sept. 14, 2008. http://www.sciencedaily.com/releases/2008/09/080910092613.htm.
(32) Bunch, J. S.; van der Zande, A. M.; Verbridge, S. S.; Frank, I. W.; Tanenbaum, D. M.; Parpia, J. M.; Craighead, . G.; McEuen, P. L. Electromechanical resonators from graphene sheets. *Science* **2007**, *315*, 490−493.
(33) Lee, C.; Wei, X.; Kysar, J. W.; Hone, J. Measurement of the elastic properties and intrinsic strength of monolayer graphene. *Science* **2008**, *321*, 385−388.
(34) Lui, C. H.; Liu, L.; Mak, K. F.; Flyn, G. W.; Heinz, T. F. H. Ultraflat graphene. *Nature* **2009**, *462*, 339−341.
(35) Dean, C. R.; Young, A. F.; Meric, I.; Lee, C.; Wang, L.; Sorgenfrei, S.; Watanabe, K.; Taniguchi, T.; Kim, P.; Shepard, K. L.; Hone, J. Boron nitride substrates for high-quality graphene electronics. *Nat. Nanotechnol.* **2010**, *5*, 722−726.
(36) Alekseev, K. N.; Erementchouk, M. V.; Kusmartsev, F. V. Direct current generation due to wave mixing in semiconductors. *Europhys. Lett.* **1999**, *47*, 595−600.
(37) Mikhailov, S. A. Theory of the giant plasmon enhanced second harmonic generation in graphene and semiconductor two-dimensional electron systems. *Phys. Rev. B* **2011**, *84*, 045432.
(38) Hendry, E.; Hale, P. J.; Moger, J. J.; Savchenko, A. K.; Mikhailov, S. A. Strong nonlinear optical response of graphene flakes measured by four-wave mixing. *Phys. Rev. Lett.* **2010**, *105*, 097401.
(39) Blake, P.; Hill, E. W.; Castro Neto, A. H.; Novoselov, K. S.; Jiang, D.; Yang, R.; Booth, T. J.; Geim, A. K. Making graphene visible. *Appl. Phys. Lett.* **2007**, *91*, 063124.

(40) Cheng, Y. C.; Zhu, Z. Y.; Schwingenschlögl, U. Doped silicene: Evidence of a wide stability range. *Europhys. Lett.* **2011**, *95*, 17005.